Radiation Vulnerability of Fiber Bragg Gratings in Harsh Environments

Adriana Morana, Sylvain Girard, *Senior Member, IEEE*, Emmanuel Marin, Claude Marcandella, Serena Rizzolo, Jocelyn Périsse, Jean-Reynald Macé, Abdelillah Taouri, Aziz Boukenter, Marco Cannas, and Youcef Ouerdane

***Abstract*—The difficulties encountered in the implementation of a temperature or strain sensor based on fiber Bragg grating (FBG) in a harsh radiative environment are introduced. We present the choices made to select both a radiation-resistant fiber in terms of transmission and also the grating inscription conditions necessary to write radiation tolerant FBGs in such fibers with a femtosecond laser. The radiation response of these gratings was also studied under radiation at dose up to 1 MGy. The comparison between Ge-free and Ge-doped fibers was highlighted.**

***Index Terms*—Fiber, fiber Bragg grating, radiation, radiation-induced attenuation (RIA), silica.**

I. Introduction

THE nuclear industry in the last decades showed an increasing interest in the sensing technology based on optical fibers. Among all the optical fiber sensors (OFSs), fiber Bragg gratings (FBGs) were the most investigated under radiation [1]; indeed, the increase of attenuation induced by ionizing radiation limits the intensity-based OFSs in harsh environments, favoring sensors whose information is encoded in wavelength measurements. The FBG sensing is based on the dependence of the Bragg wavelength (λ_B) position on external parameters, as temperature, strain and pressure [2]:

$$\lambda_B = 2 \cdot n_{\text{eff}} \cdot \Lambda \quad (1)$$

where n_{eff} is the effective refractive index of the fundamental mode and Λ is the grating period. Radiation influences the grating response in different ways. Firstly, ionizing radiation produces point defects whose absorption bands increase the optical fiber transmission losses. Even if the information on the sensing parameter is not encoded on the peak intensity, the radiation-induced attenuation (RIA) degrades the grating performance by decreasing the signal-to-noise ratio and, in some cases, losses can be so high to make it impossible to measure and detect the grating peak [3]. An easy way to reduce the total losses consists of splicing small pieces of photosensitive fibers, where the gratings can be easily written with UV based-techniques, to more radiation-resistant fibers, as suggested by Niay *et al.* [4]. Otherwise, gratings have to be written directly into radiation-resistant fibers with a F-doped silica or pure-silica core [5]. These fiber types are not as photosensitive as germanosilicate ones to classical UV lasers, as cw or pulsed in the nanosecond domain. Indeed, Albert *et al.* [6] showed that with an ArF laser at 193 nm it is possible to write FBGs with a modulation amplitude of about 10^{-5} in a pure silica core fiber (total fluence of about 18 kJ/cm^2) and with a modulation of one order of magnitude higher in a Ge-doped core fiber with a total fluence lower by a factor of 5. For this reason, a more efficient technique for the FBG inscription in Ge-free fibers was developed using the femtosecond UV or IR lasers [7].

Secondly, radiation-induced defects and density variations lead to changes in the grating period and in the refractive indices of the different grating zones, that entail changes both in the effective index and in the index modulation amplitude. Consequently, radiation induces a shift of the peak wavelength (hereafter named Bragg wavelength shift, BWS) and a reduction of the peak amplitude. The first gives rise to an error on the measurement of the sensing parameter; the second leads to a reduction of the signal-to-noise ratio. The behavior of the BWS as a function of the dose is strongly dependent on fiber composition, grating inscription conditions and pre-irradiation treatments [1], so it is necessary to test as more gratings as possible to determine the best grating for the aimed application. Since the recent discovery to write gratings with femtosecond IR laser, very few works [8] were dedicated to study the radiation sensitivity of these fs-FBGs. In spite of all the previous studies, research is still very active on this field, under the need to find radiation-resistant gratings working as strain or temperature sensors and to explain the different behaviors of the radiation-induced peak shift.

In this work, we extend our preliminary discussion [9] concerning the radiation effects induced on the transmission of different fiber types and on the Bragg peak of gratings written in these fibers by femtosecond radiation at 800 nm. Moreover, we evidence the main difference between the gratings written by UV laser or femtosecond IR radiation, not only comparing the radiation-induced shift but also investigating the defects generated during the grating inscription with confocal spectroscopy.

A. Morana, S. Girard, E. Marin, S. Rizzolo, A. Taouri, A. Boukenter, and Y. Ouerdane are with the Laboratoire H. Curien, UMR CNRS 5516, Université Jean Monnet, 42000 Saint-Etienne, France (e-mail: adriana.morana@univ-st-etienne.fr; sylvain.girard@univ-st-etienne.fr; emmanuel.marin@univ-st-etienne.fr; serena.rizzolo@univ-st-etienne.fr; abdelillah.taouri@univ-st-etienne.fr; aziz.boukenter@univ-st-etienne.fr; ouerdane@univ-st-etienne.fr).

C. Marcandella is with the CEA, DAM, DIF, F-91297 Arpajon, France (e-mail: claude.marcandella@cea.fr).

J. Périsse is with Areva NP, 69456 Lyon Cedex 06, France (e-mail: jocelyn.perisse@areva.com).

J.-R. Macé is with Tour Areva, 92084 Paris La défense Cedex, France (e-mail: jean-reynald.mace@areva.com).

M. Cannas is with the Dipartimento di Fisica e Chimica, Università di Palermo, I-90123 Palermo, Italy (e-mail: marco.cannas@unipa.it).

Digital Object Identifier 10.1109/JLT.2014.2364526

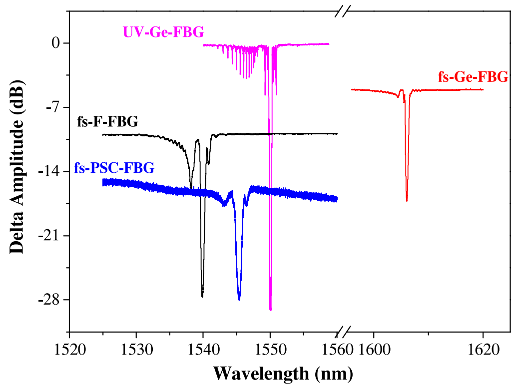

Fig. 1. Transmission spectra of the FBGs. To have a clearer graph, their zero amplitude lines were shifted by 5 dB.

TABLE I
GRATINGS' PARAMETERS

FBG	Laser power (mW)	Bragg peak		
		Wavelength (nm)	Amplitude (dB)	FWHM (nm)
UV-Ge	100	1550.045 ± 0.003	28.70 ± 0.13	0.397 ± 0.013
fs-Ge	300	1606.033 ± 0.002	12.210 ± 0.011	0.567 ± 0.002
fs-F	500	1539.736 ± 0.002	18.526 ± 0.008	0.577 ± 0.002
fs-PSC	500	1545.354 ± 0.010	12.00 ± 0.04	0.932 ± 0.013

Parameters values of the gratings. The values here reported are average of a set recorded before the irradiation start; the errors are calculated as twice the standard deviation of the set (confidence of about 96%).

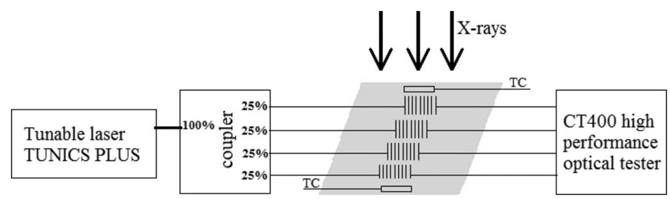

Fig. 2. Experimental setup. TC is a thermocouple.

II. EXPERIMENTAL PROCEDURE

We investigated three different types of single-mode fibers (SMF): the first is characterized by a Ge-doped core, the second one by a F-doping both in the core and in the cladding and the third fiber has a core in pure silica and a F-doped cladding (hereafter indicated as PSC fiber). All the fibers have cladding and core size diameters of 125 μm and 8–9 μm respectively.

FBGs were written in all the fiber types by an ultra-fast Ti:sapphire laser emitting pulses at 800 nm with duration of 50 fs and repetition rate of 1 kHz, through two different phase-masks. To irradiate the whole core, the focusing lens can be translated perpendicularly to the direction of light propagation at a frequency ranging between 10 mHz and 10 Hz. Moreover, in the Ge-doped fiber that is naturally photosensitive to UV light, a grating was written by using a frequency doubled cw argon-ion laser (Coherent), emitting at 244 nm (maximum power of 250 mW). Thanks to the high laser power, the grating was realized directly, without moving the fiber, by using a beam expander. However, a H_2-loading (during a week at RT and 130 bars) was performed on the Ge-doped fiber before inscription, to increase its photosensitivity, and an annealing (at 80 °C for 7 h) was necessary after the grating inscription, to remove the remaining hydrogen. In contrast with this, the fs-FBGs were neither H_2-loaded nor thermally treated after inscription. The optical fibers were mechanically stripped of the coating for the inscription and the gratings, 1 cm long, were not recoated. The transmission spectra of the gratings used in the experiment are shown in Fig. 1; the inscription conditions and the parameters of the gratings are reported in Table I.

The peak position was determined by fitting about 170 pm range of the transmission spectrum near the main dip with a third order polynomial approximation, to account for a possible peak asymmetry. The full width at half maximum (FWHM) of the Bragg peak was calculated as the distance between two points on the two sides of the central wavelength at which the amplitude is half of the maximum peak value expressed in dB.

Two different sources, Brigitte ^{60}Co facility in SCK•CEN (Mol, Belgium) and 10 keV X-ray Aracor machine at the CEA (Arpajon, France), were used to investigate the radiation response of our samples. The energy deposition mechanisms at these two energies are well known [10] and previous works using various spectroscopic techniques confirmed that both sources lead to the same defect generation mechanisms in silica-based optical fibers. Then, radiation-effects on fiber transmission and Bragg grating were studied with these two different irradiation sources because of their characteristics and accessibilities. The γ-source allows us to irradiate long length of fibers, with a dose-rate lower than 8 Gy(SiO_2)/s and a temperature (lower than 60 °C) not adjustable, but not to realize on-line tests. These, instead, can be performed on only 2 cm long fibers with the X-source, at higher dose-rate (up to 50 Gy(SiO_2)/s) decreasing the experiment time. To study the RIA, 30 m length of each fiber type was γ-irradiated up to total dose of 10 MGy. Permanent radiation induced damages were characterized at room temperature (RT) some months after irradiation, by performing loss measurements at 1550 nm with an optical time domain reflectometer (OTDR FTB-74000E from Exfo) [11]. To determine the origin of this attenuation, spectral measurements were realized by the cut-back method. Transmission spectra were recorded with two white light sources, a spectrometer QE65000 from Ocean Optics for the visible range, between 400 and 700 nm, and an OSA from Yokogawa for the IR range, between 1200 and 1600 nm.

To investigate the radiation sensitivity of the gratings, X-ray irradiations were performed at RT (around 25 °C) with dose-rate of 50 Gy/s and accumulated dose of 1 MGy. Contrary to the γ-system, the irradiation setup is also provided by a high-performance Temptronic thermo-chuck to well control the temperature. During irradiation, four gratings were fixed stress-free on the heating plate of the irradiation system and their transmission spectra were recorded, as shown in Fig. 2, in parallel by using a tunable laser Tunics Plus source from NetTest and the CT400 high performance optical tester from Yenista Optics. The wavelength resolution was fixed to 1 or 2 pm, for gratings

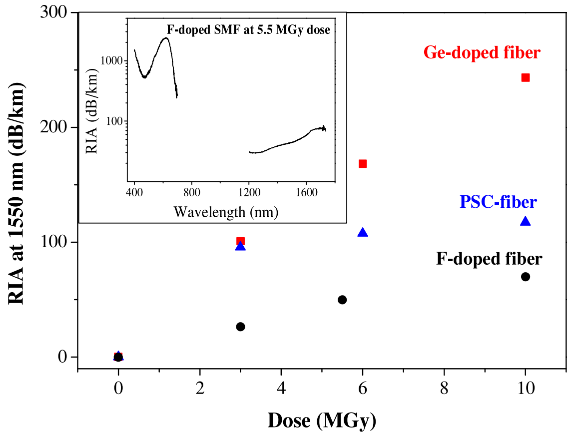

Fig. 3. RIA at 1550 nm as a function of the dose for the F-doped (black circles), PSC (blue triangles) and Ge-doped (red squares) SMFs. In the inset, attenuation spectrum induced at 5.5 MGy dose in the F-doped fiber.

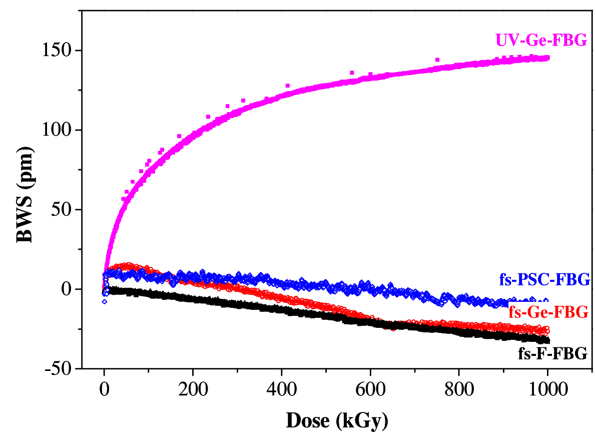

Fig. 4. Radiation-induced BWS as a function of the dose, dose-rate being 50 Gy/s.

written in the F-doped and PSC fibers or in the Ge-doped fibers, respectively.

The temperature changes, to which the gratings were subjected, were monitored by two thermocouples fixed on the same heating plate on both sides of the gratings at a distance of about 1 mm. Indeed, during the irradiation a temperature increase (lower than 4 °C) was recorded; so, to isolate only the radiation-induced BWS, the temperature-induced contribution was taken into account, once the temperature sensitivity was known. This coefficient was determined by varying temperature from 20 °C to 40 °C just before irradiation. The temperature sensitivity is ∼10 pm/°C for both gratings written in the Ge-doped fiber, independently of the laser wavelength, and ∼15 pm/°C for those performed in the Ge-free fibers.

The grating photo-inscription effects were studied via confocal micro-photoluminescence (PL) and micro-Raman measurements by using a LabRam Aramis (Jobin-Yvon) spectrometer, equipped with a He-Cd ion laser probe emitting at 3.82 eV (325 nm), a x40 objective and microtranslation stages. The corresponding spatial resolution was about 5 μm.

III. Results

A. Gamma-RIA

Fig. 3 reports the RIA values recorded some months after irradiation with the OTDR at 1550 nm. This permanent attenuation increases with increasing dose for all the fibers. For the Ge-doped fiber the RIA dependence on the dose is described by a power law [12], whereas for the Ge-free fibers a clear saturating behavior is observed. The inset of Fig. 3 shows the attenuation spectrum recorded with the cut-back technique in the F-doped SMF irradiated at 5.5 MGy dose. Despite the spectra missing part, due to the range of the two detectors, the RIA curve consists of three contributions: an UV-tail, at least an absorption band around 600 nm and an IR-absorption which increases with increasing wavelength.

B. X-Rays Induced Changes in the Bragg Peak

Fig. 4 shows the radiation-induced BWS of the gratings listed above.

The results obtained for the FBG written with UV light in the Ge-doped fiber (UV-Ge-FBG) are consistent with those reported in literature [1]: the Bragg peak red-shifts with an initial fast increase followed by a slower tendency to saturate. The peak shift should saturate at a dose higher than 1 MGy, around a value slightly larger than 150 pm. For the three fs-FBGs, instead, the general effect is a peak blue-shift. However, an initial red-shift is observed for the gratings written in the PSC and Ge-doped fibers up to the dose of about 23 and 56 kGy, respectively, at which the inversion of the shift direction occurs. The BWS towards the blue does not show a saturating behavior up to 1 MGy dose; moreover, the slope of the blue shift is larger for the Ge-doped FBG than for the Ge-free FBGs, by a factor ∼2 (–0.05 pm/kGy against -0.03 pm/kGy for the F-doped core fiber and -0.02 pm/kGy for the PSC fiber). At the accumulated dose of 1 MGy, the BWS is about 10 pm for the grating written in the PSC fiber, 24 pm in the Ge-doped fiber and 32 pm in the F-doped fiber.

The radiation-induced changes of the peak amplitude are within 0.2 dB, which corresponds to only 1% of the initial value. Whereas a clear trend cannot be observed for the UV-grating, the fs-FBGs' amplitude initially increases and then starts decreasing at different values of the accumulated dose with respect to the BWS. The variation of the peak FWHM is always lower than 10 pm, within 3% of its initial value. As an example, Fig. 5 reports the changes observed on the grating written in the F-doped fiber. This FBG does not show a direction inversion for the BWS but it does for the peak amplitude and width, which have similar behavior.

C. Laser Effects During the Grating Inscription

Spatial distribution of defects induced by the writing laser light was studied over the transverse fiber section, thanks to the confocal micro-luminescence setup.

Typical PL spectra emitted from the core center of the pristine Ge-doped SMF and the UV-Ge-FBG are reported in the inset of Fig. 6 under an excitation probe laser source at 325 nm. These results highlight the effects of UV laser photo-inscription on the Ge doped fiber. The PL band peaked at 400 nm is associated with germanium lone pair centers (GLPC) [13]; whereas

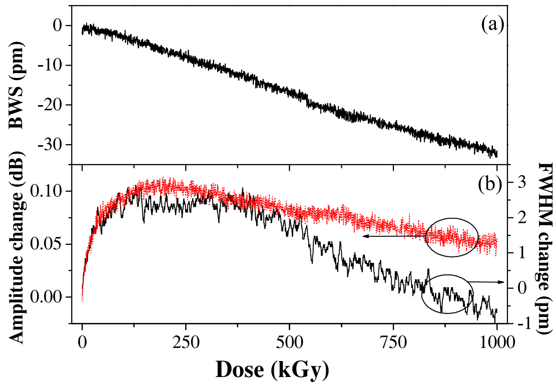

Fig. 5. Radiation-induced changes for the fs-FBG written in the F-doped fiber: (a) the Bragg wavelength decreases with dose; (b) the peak FWHM (continuous black line) and amplitude (dotted red line) initially increase and then decrease.

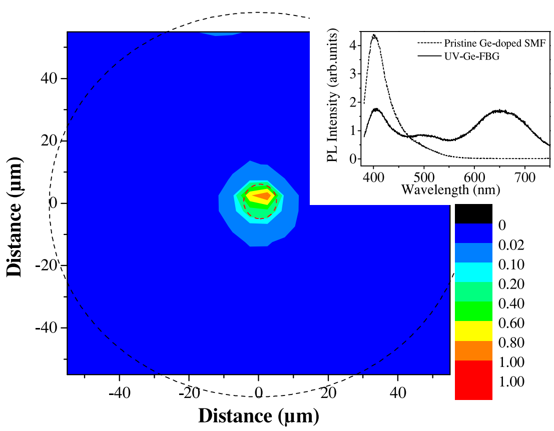

Fig. 6. Normalized map of the PL intensity around 650 nm in the UV-Ge-FBG. The inset shows the PL spectrum emitted under excitation at 325 nm from the center of the pristine Ge-doped fiber (dotted line) and the UV-Ge-FBG (continuous line). The small dashed red circle represents the core zone ($\sim$9 μm diameter) and the large dashed black circle represents the cladding.

the band around 650 nm is related to nonbridging hole oxygen centers (NBOHC) [14] linked to both Ge and Si atoms. As shown in this figure, the UV irradiation generates NBOHCs, whose concentration increases, and reduces the GLPCs reservoir concentration. Similar results have been already obtained on X-irradiated Ge-doped fibers [15] involving possible photo-induced processes for the conversion mechanisms of the Ge-related defects. Fig. 6 depicts the intensity distribution of the 650 nm PL over the Ge-doped fiber transverse cross section and shows that the NBOHCs induced during the grating writing are concentrated mainly in a symmetrical area around the core.

Concerning the defects created during the FBG inscription with femtosecond IR-radiation, we report the results obtained on the fs-F-FBG; in such a way we avoid to study defects peculiar to the Ge-doping. The inset of Fig. 7 points out that the main PL induced by the IR laser (under excitation at 325 nm) is located around 650 nm, associated with NBOHCs. In contrast with the UV writing, the distribution of the IR laser induced centers is not symmetrical, as shown in Fig. 7: the defects are concentrated in the core and even in an area along the laser direction.

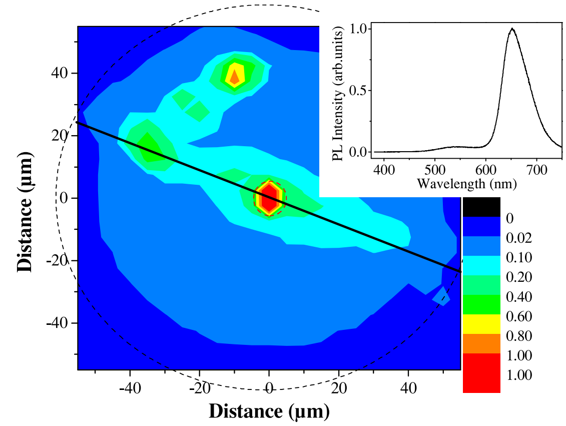

Fig. 7. Normalized map of the PL intensity around 650 nm in the fs-F-FBG. The inset shows the PL spectrum emitted from the center of the fs-F-FBG under excitation at 325 nm. The small dashed red circle represents the core zone ($\sim$9 μm diameter) and the large dashed black circle represents the cladding.

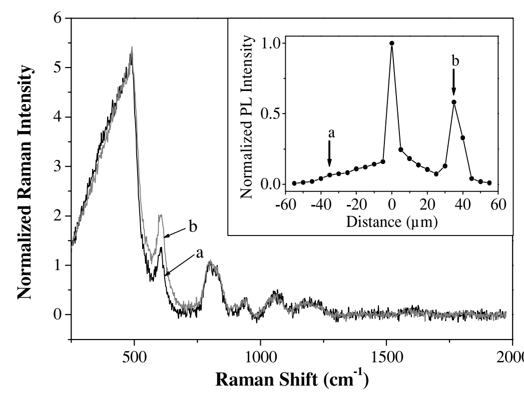

Fig. 8. Raman spectra recorded in two points at the same distance from the core center along the fiber diameter reported in black in the previous figure. The point b (grey curve) has been irradiated by the IR laser, whereas the point a (black curve) has not, as it can be observed by the values of the PL intensity at 650 nm PL along the diameter, reported in the inset.

IR laser causes also structural changes. To observe them, we consider the fiber diameter indicated in Fig. 7 with the black straight line. The inset of Fig. 8 shows the intensity of the 650 nm PL band along this diameter. As it is evident from the high value of the PL intensity, the point "b" has been irradiated, whereas the other point at the same distance from the core, indicated with "a", has not. Since the dopant concentration is identical in the two points, they should be characterized by the same Raman spectrum. Instead, despite the low signal-to-noise ratio of the spectra, Fig. 8 highlights an increase of the band around 605 cm^{-1}, known as D_2 band and assigned to the oxygen-breathing mode associated with three-membered SiO_4 rings [16]. This is an evidence of the structural changes induced by fs IR-radiation.

IV. Discussion

In the first part of this work we demonstrated that it is advantageous to write gratings in the IR spectral range, since the IR-RIA is lower than that induced in the UV-Visible spectral range by at least one order of magnitude, as shown in the inset of Fig. 3. The same figure highlights that the 1550 nm RIA in the Ge-doped fiber is higher than in the Ge-free one. Among the analyzed samples, the most radiation-resistant is the F-doped fiber, whose RIA saturates around 70 dB/km at the γ-dose of 10 MGy.

Unlike most of the absorption bands in the UV-visible region of the spectrum, the origin of the IR-RIA is not clear yet; only very few studies deal with this IR band. Chernov [17] attributed to self-trapped holes a NIR-band peaked at a wavelength longer than 1500 nm. Since we record only the tail of an IR band, we cannot determine the spectral parameters of this absorption band to confirm its attribution. Moreover, from the shape of the absorption around 600 nm we cannot affirm the presence of another band peaked at 660 nm and associated to the same defects [18].

The RIA limits the OFS performance; indeed, even if the FBG-based sensor allows only localized measurements, more gratings can be written in series inside a same fiber to determine the sensing parameter in different points along the fiber length, e.g. about ten gratings could be written along 100 m long fiber for civil nuclear applications. Concerning the gratings, the important condition that must be verified is not to overlap the spectral ranges in which the peak of each FBG can vary, for example the peaks' positions must be spaced few nm, if the gratings are temperature sensors working from RT to 100 °C. The fiber, instead, must be characterized by a reduced RIA value to allow the signal transmission along the whole fiber length and then the monitoring of all the gratings written in the same sample. As an example, we take into account a 100 m long fiber inside which ten gratings are written at a space distance of 10 m from each other and an acquisition system with an optical budget of 10 dB. At an irradiation dose of 10 MGy, the signal will be attenuated at the fiber end by 24 dB for the Ge-doped fiber, which means that it will propagate for less than half distance, i.e. 41 m, and therefore only the first four gratings will be tested. For the F-doped fiber, instead, the signal attenuation along the whole fiber length will be around 7 dB and all the sensors could be checked at the total dose of 10 MGy.

Secondly, we performed the irradiation tests on gratings and pointed out that fs-FBGs are less sensitive to radiation than classical UV-gratings. The main cause is the H_2-loading of the fiber before the grating inscription with UV light; nevertheless, it is necessary to make the fiber more photosensitive. The increase of the radiation-sensitivity with the hydrogenation has been already observed [19] and associated with the radiolytic rupture of OH-bonds [20].

Even if the BWS induced in the UV-FBG is higher than in the fs-gratings, it shows a saturating behavior, whereas the peak shift of the fs-FBGs does not seem to saturate up to 1 MGy accumulated dose. The main radiation effect on the peak of these gratings is a blue-shift. A comparable behavior was observed by Henschel *et al.* on similar fs-FBGs [8]: the BWS induced at the accumulated dose of 1 MGy is between -10 pm and $+15$ pm, lower than in our case. Apart the inscription conditions, one of the main causes of this difference is probably related with the different irradiation conditions: we used a higher dose-rate than in the experiment performed by Henschel *et al.* in their paper, 50 Gy/s against 2 Gy/s. For the classical UV-FBGs, Fernandez *et al.* have inferred that the higher dose-rate, the bigger the radiation-induced BWS [21]. Assuming the same behavior for the fs-FBGs, the higher dose-rate should be the cause of the larger BWS here reported. Moreover, we have to note another important difference between our fs-gratings and those reported in literature: ours did not withstand any thermal treatments after inscription. The effect of a pre-irradiation thermal treatment on the radiation-response is not clear yet and it depends on several parameters, as those of the inscription and of the treatment itself. By comparing the radiation-induced BWS of our gratings with those of Henschel *et al.* [8], it is likely that the annealing changes the dose and BWS values at which the shift direction occurs, and it could also reduce the BWS.

To try to understand the differences of both used inscription techniques, thanks to the confocal micro-luminescence, we studied the defects induced in the fiber by the grating inscription process. Independently of the writing laser source, the induced defects are mainly concentrated in the core region, indeed during the grating inscription the laser is focused into the fiber core. The light focalization that is simple for UV lasers becomes more complicated for the fs-gratings, because of the critical alignment between laser and fiber. This operation is realized by connecting one fiber end to a spectrometer working in the visible spectral domain to record online the emitted spectra with PL bands of defects induced by the IR-radiation inside the fiber and optimizing the interaction between incoming laser and fiber. During this procedure, the laser power is fixed at a lower value than during the inscription in order to avoid possible structural modifications of the fiber.

Figs. 6 and 7 showed the differences: the UV light generates defects only in a symmetrical area around the fiber core zone, whereas the defects produced by the fs IR-radiation are present in the fiber core and in an area along the laser direction. This asymmetry has been already observed for the fs-FBGs by Troy *et al.* [22]. Nevertheless, we took advantages of this asymmetry to study the structural changes induced by the fs laser, by easily comparing two small regions of the fiber (area of 5 μm $\times$ 5 μm) at the same distance from the core center but whose one was irradiated and the other was not. This lets us highlight the D_2 band increase induced by the fs IR-laser. Several research groups studied the effects induced by femtosecond IR laser in silica [23] and demonstrated that they are consistent with a densification process; indeed the main induced changes in the Raman spectra are the shift to higher frequencies and the width decrease for the main 440 cm^{-1} band and the intensity increase for the D_2 band. No result has been presented in literature, to our knowledge, about the effects of the fs IR-radiation on fibers. In our case, a radiation influence on the D_2 band is clearly observed in Fig. 8; but, because of the low signal-to-noise ratio, it is not possible to know if the radiation causes other small changes, as a shift of the main band, confirming the hypothesis of densification, or if the D_2 band increase is the only one and it is due to an increase of the stress inside the fiber. However, what is important to note is that structural modifications of the glass or stress redistribution can be induced during the fs-FBG writing and they could be crucial to determine the influence of radiation or thermal treatment on the grating response. For example, whereas a pre-irradiation thermal treatment increases the radiation sensi-

TABLE II
RADIATION-INDUCED ERROR

FBG	Temperature error at 1 MGy dose
UV-Ge	+14 °C
fs-Ge	−2.2 °C
fs-F	−2.3 °C
fs-PSC	−0.7 °C

Error on the temperature measurement by using the FBGs as temperature sensors in radiative environments at the accumulated dose of 1 MGy.

tivity of the UV-gratings by restoring precursors, as observed by Gusarov *et al.* [20], a different temperature effect on the radiation-resistance could be obtained for the fs-gratings, depending on its effects on the structure or stress distribution. For this reason, a study of the radiation resistance of the fs-FBGs as a function of the temperature of a pre-irradiation annealing has been recently realized by our research group [24].

Based on the above discussion, the research on radiation-resistant gratings is still of interest: very low values of the radiation-induced BWS must be obtained to use the gratings in harsh environments as strain or temperature sensors, because the BWS entails an error on the sensing parameter measurement. For example, for our gratings, if they are used as temperature sensors, the BWS induced at 1 MGy dose corresponds to an error of around 2 °C on the temperature measurement for the worst gratings, as reported in Table II. Moreover, this error is reduced to less than 1 °C for the grating written in the PSC fiber.

V. CONCLUSION

In this work we show the preliminary study that has to be performed to determine and identify both the adapted fiber and the Bragg grating photo-inscription conditions to realize a strain and/or temperature sensor suitable for a harsh environment. The F-doped SMF showed the lowest RIA value at 1550 nm among the analyzed samples at an accumulated dose of 1 MGy. The choice of a Ge-free fiber promotes the fs-radiation, as the one we used operating at 800 nm, for the grating inscription. On the contrary of the RIA, no strong dependence of the fs-FBGs' radiation sensitivity on the fiber composition was observed. Moreover, the blue-shift of the Bragg peak at 1 MGy dose corresponds to an error on the temperature measurement lower than 2.5 °C.

REFERENCES

[1] A. I. Gusarov and S. K. Hoeffgen, "Radiation effects on fiber gratings," *IEEE Trans. Nucl. Sci.*, vol. 60, no. 3, pp. 2037–2053, Jun. 2013.

[2] K. O. Hill and G. Meltz, "Fiber Bragg grating technology fundamentals and overview," *J. Lightw. Technol.*, vol. 15, no. 8, pp. 1263–1276, Aug. 1997.

[3] S. A. Vasiliev, E. M. Dianov, K. M. Golant, O. I. Medvedkov, A. L. Tomashuk, V. I. Karpov, M. V. Grekov, A. S. Kurkov, B. Leconte, and P. Niay, "Performance of Bragg and long-period gratings written in N- and Ge-doped silica fibers under γ-radiation," *IEEE Trans. Nucl. Sci.*, vol. 45, no. 3, pp. 1580–1583, Jun. 1998.

[4] P. Niay, P. Bernage, M. Douay, F. Fertein, F. Lahoreau, J. F. Bayon, T. Georges, M. Monerie, P. Ferdinand, S. Rougeault, and P. Cetier, "Behavior of Bragg gratings, written in germanosilicate fibers, against γ ray exposure at low dose rate," *IEEE Photon. Technol. Lett.*, vol. 6, no. 11, pp. 1350–1352, Nov. 1994.

[5] S. Girard, J. Kuhnhenn, A. Gusarov, B. Brichard, M. Van Uffelen, Y. Ouerdane, A. Boukenter, and C. Marcandella, "Radiation effects on silica-based optical fibers: Recent advances and future challenges," *IEEE Trans. Nucl. Sci.*, vol. 60, no. 3, pp. 2015–2036, Jun. 2013.

[6] J. Albert, M. Fokine, and W. Margulis, "Grating formation in pure silica-core fibers," *Opt. Lett.*, vol. 27, no. 10, pp. 809–811, May 2002.

[7] S. J. Mihailov, C. W. Smelser, D. Grobnic, R. B. Walker, P. Lu, H. Ding, and J. Unruh, "Bragg gratings written in all-sio$_2$ and Ge-doped core fibers with 800-nm femtosecond radiation and a phase mask," *J. Lightw. Technol.*, vol. 22, no. 1, pp. 94–100, Jan. 2004.

[8] H. Henschel, D. Grobnic, S. K. Hoeffgen, J. Kuhnhenn, S. J. Mihailov, and U. Weinand, "Development of highly radiation resistant fiber Bragg gratings," *IEEE Trans. Nucl. Sci.*, vol. 58, no. 4, pp. 2103–2110, Aug. 2011.

[9] A. Morana, S. Girard, E. Marin, C. Marcandella, J. Périsse, J.-R. Macé, A. Boukenter, M. Cannas, and Y. Ouerdane, "Radiation hardening of FBG in harsh environments," presented at the Int. Conf. Opt. Fiber Sensors, Santander, Spain, 2014.

[10] P. Paillet, J. R. Schwank, M. R. Shaneyfelt, V. Ferlet-Cavrois, R. L. Jones, O. Flament, and E. W. Blackmore, "Comparison of charge yield in MOS devices for different radiation sources," *IEEE Trans. Nucl. Sci.*, vol. 49, no. 6, pp. 2656–2661, Dec. 2002.

[11] H. Henschel, O. Kohn, and H. U. Schmidt, "Radiation induced loss measurements of optical fibres with optical time domain reflectometers (OTDR) at high and low dose rates," presented at the Europ. Conf. Radiation and its Effects on Devices and Systems, La Grande-Motte, France, 1991.

[12] M. Van Uffelen, "Modélisation de systèmes d'acquisition et de transmission à fibres optiques destinés à fonctionner en environnement nucléaire," Ph.D. dissertation, U.F.R Scientifique d'Orsay Paris, Univ. de Peris XI, Peris, France, 2001.

[13] L. Skuja, "Isoelectronic series of twofold coordinated Si, Ge, and Sn atoms in glassy SiO_2: A luminescence study," *J. Non-Cryst. Solids*, vol. 149, pp. 77–95, Oct. 1992.

[14] L. Skuja, "The origin of the intrinsic 1.9 eV luminescence band in glassy SiO_2," *J. Non-Cryst. Solids*, vol. 179, pp. 51–69, Nov. 1994.

[15] A. Alessi, S. Girard, M. Cannas, S. Agnello, A. Boukenter, and Y. Ouerdane, "Evolution of photo-induced defects in Ge-doped fiber/preform: Influence of the drawing," *Opt. Exp.*, vol. 19, no. 12, pp. 11680–11690, Jun. 2011.

[16] G. S. Henderson, D. R. Neuville, B. Cochain, and, L. Cormier, "The structure of GeO_2-SiO_2 glasses and melts: A Raman spectroscopy study," *J. Non-Cryst. Solids*, vol. 355, pp. 468–474, Mar. 2009.

[17] P. V. Chernov, "Spectroscopic manifestations of self-trapped holes in silica," *Phys. Stat. Sol.*, vol. B115, pp. 663–675, 1989.

[18] D. L. Griscom, "γ-ray-induced visible/infrared optical absorption bands in pure and F-doped silica-core fibers: Are they due to self-trapped holes?," *J. Non-Cryst. Solids*, vol. 349, pp. 139–147, Nov. 2004.

[19] A. I. Gusarov, D. S. Starodubov, F. Berghmans, O. Deparis, Y. Defosse, A. Fernandez Fernandez, M. Décreton, P. Mégret, and M. Blondel, "Comparative study of MGy dose level γ-radiation effect on FBGs written in different fibres," in *Proc. Int. Conf. Opt. Fiber Sensors*, Kyongju, Korea, 1999, pp. 608–611.

[20] A. Gusarov, S. Vasiliev, O. Medvedkov, I. Mckenzie, and F. Berghmans, "Stabilization of fiber Bragg gratings against gamma radiation," *IEEE Trans. Nucl. Sci.*, vol. 55, no. 4, pp. 2205–2212, Aug. 2008.

[21] A. Fernandez Fernandez, B. Brichard, F. Berghmans, and M. Décreton, "Dose-rate dependencies in gamma-irradiated fiber Bragg grating filters," *IEEE Trans. Nucl. Sci.*, vol. 49, no. 6, pp. 2874–2878, Dec. 2002.

[22] N. Troy, C. W. Smelser, and D. M. Krol, "Role of hydrogen loading and glass composition on the defects generated by the femtosecond laser writing process of fiber Bragg gratings," *Opt. Mater. Exp.*, vol. 2, no. 11, pp. 1663–1670, Nov. 2012.

[23] K. Mishchik, "Transformation photo-assistée de diélectriques pour l'optique par laser à impulsions ultra-brèves: Etudes des mécanismes microscopiques," Ph.D. dissertation, Laboratoire H. Curien, Univ. Jean Monnet, Saint Etienne, France, 2012.

[24] A. Morana, S. Girard, E. Marin, C. Marcandella, P. Paillet, J. Périsse, J.-R. Macé, A. Boukenter, M. Cannas, and Y. Ouerdane, "Radiation tolerant fiber Bragg gratings for high temperature monitoring at MGy dose levels," *Opt. Lett.*, vol. 39, no. 18, pp. 5313–5316, Sep. 2014.

Authors' biographies not available at the time of publication.